Investigation of the intra-annual variability of the North Equatorial Counter Current/ North Brazil Current eddies and of the instability waves of the North tropical Atlantic Ocean using satellite altimetry and Empirical Mode Decomposition

Jean-Luc Mélice & Sabine Arnault

LOCEAN-IPSL, UMR CNRS/IRD/UPMC/MNHN, Université Pierre et Marie Curie, Paris , France (jlmelice@locean-ipsl.upmc.fr)

The intra-annual variability of the tropical Atlantic Ocean north of the Equator is investigated with satellite altimetry mean sea level anomalies (SLA) data, and with an algorithm based on Empirical Mode Decomposition method. Two regions of high variability are identified:

The first region, between 3°N-12°N, is characterized by the presence of westward propagating eddies linked to the North Brazil Current retroflection in the vicinity of the Brazilian coast. They show a strong annual cycle. Our EMD algorithm points out that this signal is frequency modulated shifting from large lengthscale structures in October to smaller ones in March. Consequently, the number of 'eddies' per year can be aliased, according to the time and location of sampling, and can impact the percentage they explain of the inter-hemispheric exchange of mass and heat associated with the meridional overturning circulation's upper limb. A scenario concerning this dynamics is proposed.

The second region reveals the presence of westward propagating instability waves centered north of the Equator (3°N-7°N) between 50°W-10°W. These instability waves are also frequency modulated and show a strong seasonal cycle with maximum amplitude around August.

Data and methods

Satellite Sea Level Anomalies (SLA) data

- AVISO SSALTO/DUACS SLA merged products *(http://www.aviso.oceanobs.com)*. Our analyses are performed on the anomalies of the SLA signals.
- Resolutions: weekly from October 1992 to September 2015, 1/3°x1/3° from 20°N to 20°S, 60°W to 20°E.

Methods

- Empirical Mode Decomposition (EMD), Hilbert Transform (HT), Complex Empirical Orthogonal Functions (C-EOF)

EOF of Sea Level Anomalies (SLA) on maximum standard deviation ridge

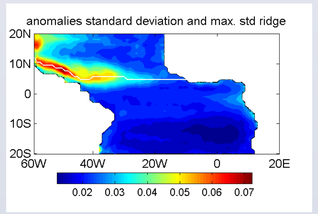

Fig. 1: Std dev (m) of the SLA , and maximum std dev ridge (white line).

Fig. 1
The region of maximum standard deviation of the SLA is concentrated between 3°N and 12°N.

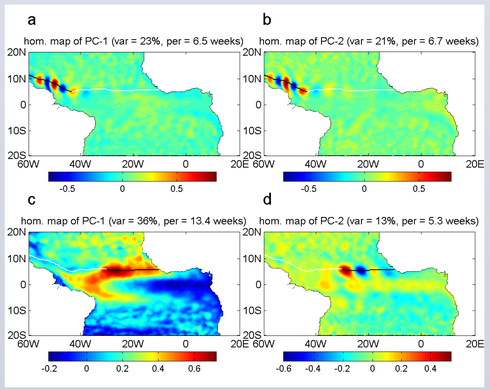

Fig. 2: (a) Homogeneous correlation map of the PC of the first EOF of the SLA restricted on the ridge of Fig. 1 from 60° to 43°W (black line). (b) As in (a), but for EOF-2. (c), (d) As in (a), (b), but from 30°W to 10°W.

Fig. 2
The PCs 1-2 (homogeneous maps) in (a,b) are in quadrature. They show propagating "eddies". We suggest that these are instabilities generated by the retroflection of the North Brazil Current (NBC) to the North Equatorial Counter Current (NECC) in the vicinity of the Brazilian coast.
The PCs 1-2 in (c,d) show the presence of two different processes at the same latitude, which could be linked to Rossby (and Kelvin equatorward) waves for PC-1 (c), and instability waves for PC-2 (d). Their periods are 13.4 (low frequency LF) and 5.3 (high frequency HF) weeks, respectively.
These two processes can be analyzed with precision if the SLA signals are decomposed in their LF in and HF components. It is also the case for the other processes investigated in this study.
For this purpose, we have developed an EMD-based algorithm which is very efficient for separating automatically (without any a priori cutoff period) the LF and HF components. As they are asymptotic, their amplitude (envelope) and frequency modulations can be estimated.

Frequency characteristics of the SLA between 3°N-12°N

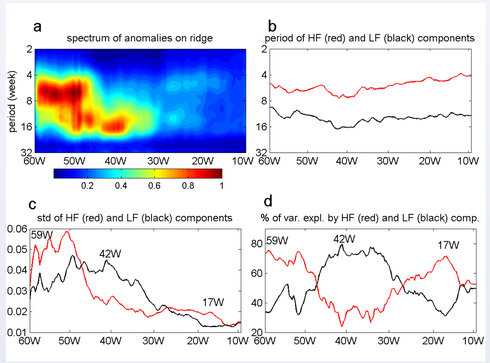

Fig. 3: Frequency characteristics of the SLA on the ridge of Fig. 1: (a) spectrum of the SLA. (b) period and (c) std dev of the HF (red) and LF (black) components. (d) % of variance of the sum of the HF and LF components explained by the HF (red) and LF (black) components.

Fig. 3
The SLA on the ridge of maximum std dev (Fig. 1a) are analyzed in the frequency domain.
The spectra in (a) shows the presence of HF and LF components. The signals are decomposed in their HF and LF components via the EMD-based algorithm. Their periods are displayed in (b).
The signals ('eddies or rings') near the Brazilian coast around 59°W are mainly composed of HF components while those around 42°W are mainly composed of LF components (c,d). The signals ('instability waves') around 17°W are mainly composed of HF components (c,d).

Characteristics of the 'rings' linked to the NBC/NECC and of the instability waves

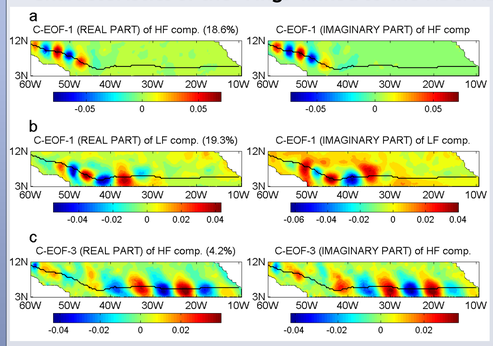

Fig. 4: (a) real and imaginary parts of the first C-EOF of the SLA HF components between 3°N and 12°N. The ridge of Fig. 1 is superimposed (black line). (b) same as (a) but for the LF components. (c) same as (a) but for the third C-EOF of the HF components.

Fig. 4
The characteristics of the 'eddies' linked to the NBC/NECC and of the 'instability' wave are investigated with the C-EOF. The patterns of the real and imaginary parts are in quadrature, indicating propagations. Their speed is estimated from the C-EOF properties.
The first C-EOFs shows that the HF structures (a) are limited to West of 45°W, and that the LF ones (b) extend from 30°to 55°W. The HF westward propagating structures ('eddies') have a diameter of ~250 km at 59°W (a), and LF westward propagating ones ('rings') have a diameter of ~500 km at 42°W (b). The third C-EOF (c) shows the presence of westward propagating structures ('insability waves') from 10° to 35°W, with a lengthscale of ~1000 km. The mean speed of the propagations (in cm/s), is 17 for the coastal 'eddies', 7-11 for the LF 'rings', and 34-41 for the 'instability waves'.

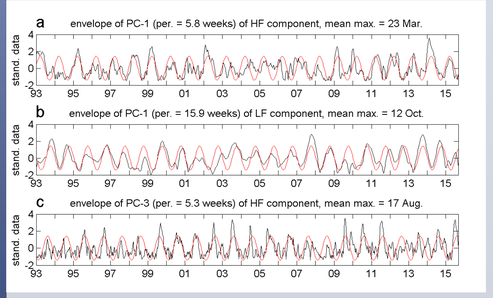

Fig. 5: (a) to (c): envelopes (black) of the PCs of the C-EOFs in Fig. 3, and fitted sine wave with a one year period (red).

Fig. 5
The envelopes of the PCs of the C-EOFs in Fig. 4 show a seasonal cycle. The envelope of PC-1 of the HF component (a) is maximum in March while the envelope of PC-1 of the LF component (b) is maximum in October. This shows that the signals ('rings') are frequency modulated: they are composed of oscillations shifting from LF in October to HF in March. Consequently the number of the NBC/NECC 'rings' varies: if we consider all values above 0.8 std dev, the mean number of rings is 5/year for PC-1 of the HF component (a), and 3/year for PC-1 of the LF component (b). The instability waves also shows a strong seasonal cycle with maximum amplitude around August (c).

Discussion

a. *Western NBC/NECC region and rings*

➢ We found a difference in terms of HF and LF structures:
- HF located west of 45°W, dominant in March, speed = 14 cm/s, zonal wavelength: ~500-600 km.
- LF located between 30-55°W, dominant in October, speed = 7-11 cm/s, meridional and zonal wavelengths : ~1050, and ~700-1000 km, respectively.

➢ Our results are in agreement with the model simulation of Jochum and Malanotte-Rizzoli [2003] (1):
- The NBC retroflects in fall and produces Rossby waves with phase speed of ~9-13 cm/s, a meridional wavelength of ~1200 km, and a zonal wavelength of 700-900 km.
- The NECC slows or even reverses in spring, the Rossby waves become westward.
- The Rossby waves are advected eastward by the NECC until 35°W, and then dissipate.
- They reflect at the Brazilian coast, creating anticyclones which intensify as they propagate NW and become NBC rings.
- Our LF signals between 35°-55°W, with maximum activity in October, corresponds to the retroflecting NBC Rossby waves (first mode).
- The HF component evolution describes the wave reflection along the Brazilian coast and the eddy formation that results, peaking now in March.

➢ According to LeBlond and Mysak [1978] (2), an incident Rossby wave with wavelength of 700-900 km, reflects with a wavelength of 400-500 km, and a group velocity northwestward along the Brazilian coast. This is close to our results with an incident zonal wavelength of ~700-1000 km (Fig. 4b) and an reflected one of ~500-600 km (Fig. 4a). To our knowledge, it is the first time that such sequence is evidenced using satellite data.

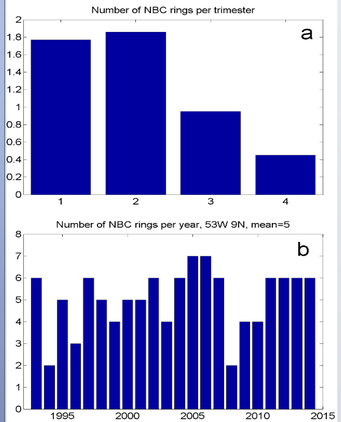

Fig. 6: (a) average number of HF rings per trimester observed from our computations at 53°W, 9°N. (b) number of HF rings per year observed from our computations at 53°W, 9°N.

Fig. 6
We assume that the HF components are a better indicator of NBC rings than the LF ones. In Fig. 6, we combined the 2 first C-EOFs obtained on the HF component of the SLAs to reconstruct the 'NBC ring' signal at 53°W, 9°N, which was the location of one of the North Brazil Current Rings Experiment discussed for instance by Johns et al. [2003] (3). Fig. 6 a and b give the mean number of rings obtained per trimester then per year after this reconstruction.
The HF signal presenting a dominant period in March, the ring activity is dominant during the 2 first trimesters, as expected. Nearly 4 rings can be identified during the first semester of a mean year. However, there is a large interannual variability as the number of rings per year varies from 2 (in 1994 and 2008) to 7 (in 2005 and 2006 for instance).
Johns et al. [2003] mentioned 8-9 rings crossing this mooring between November 1998 and June 2000. We obtain the same number in our HF SLA component at that location. These rings are in phase with those numbered 1-4 then 9-11 in their Table 2. The major discrepancy is due to the absence of the ring n°7 in October-November 1999 in our HF SLAs. But we have a strong signal in the LF component at that time (not shown). Thus from our results, Johns et al. [2003]'s ring n°7 is mostly due to a wave meander of the NBC retroflection into the NECC than a 'NBC ring'.

b. TIW region

The waves between 10°W and 50°W (Fig. 4c) show a seasonal cycle peaking around August (Fig. 5c). Their lengthscale is ~1000 km, their period is 5.3 weeks, and their mean propagation speed is 38 cm/s. These features are characteristic of the TIWs. Qiao and Weisberg [1995] (4) present a summary of TIW observations in the Atlantic and Pacific Oceans. The reported estimates generally show westward propagation in summer and fall with period, zonal wavelength and phase speed centered about 20-40 days, 600-1000 km and 30-50 cm/s, respectively. This is in agreement with our values. We also show that the TIWs are distinct from the western region LF (period = 15.9 weeks) instabilities, peaking around October (Figs. 4b, 5b).

(1) Jochum, M., P. Malanotte-Rizzoli, and A. Busalacchi (2004), Tropical instability waves in the Atlantic Ocean, *Ocean Modell.*, 7, 145-163, doi:10.1016/S1463-5003(03)00042-8.

(2) LeBlond, P.H. and L.A. Mysak, (1978), Waves in the Ocean. Elsevier, 602 pp.

(3) Johns, W.E., R.J. Zantopp, and G.J. Goni (2003), Cross-gyre transport by North Brazil Current rings. In: *Interhemispheric Water Exchange in the Atlantic Ocean*, Goni G.J. and P. Malanotte-Rizzoli (Ed.) , Elsevier Oceanography Series, 68, 411-441.

(4) Qiao, L., and R.H. Weisberg (1995), Tropical instability wave kinematics: Observations from the Tropical Instability Wave Experiment. *J. Geophys. Res.*, 100, 5, 8677-8693, doi:10.1029/95JC00305.

Acknowledgements. This study was funded by the French CNES (Centre National d'Etudes Spatiales) and the IRD (Institut de Recherche pour le Développement) organizations. Ssalto/Duacs altimeter products were produced by Ssalto/Duacs and distributed by Aviso, with support from CNES (http://www.aviso.oceanobs.com/duacs/). J.-L. Mélice and S. Arnault are supported by IRD. This work is in press in *J. Atmospheric Ocean. Tech.*, doi:10.1175/JTECH-D-17-0032.1